Moroccan Journal of Chemistry
ISSN: 2351-812X
http://revues.imist.ma/?journal=morjchem&page=login
Koulou & al. / Mor. J. Chem. 8 N°1 (2020)157-166

Synthesis of new epoxy glucose derivatives as inhibitor for mild steel corrosion in 1.0 M HCl: DMol3 theory and molecular dynamics simulation study: Part-2

A. Koulou[(a)], F. Benhiba[(b, e)], M. Rbaa[(c)], N. Errahmany[(a)], Y. Lakhrissi[(c)], R. Touir[(d)], B. Lakhrissi[(c)], A. Zarrouk [(e)], M. S. Elyoubi[(a)]

[(a)] Materials Engineering and Environment Laboratory: Modeling and Application, Faculty of Science, University Ibn Tofail P.O. Box 133-14000, Kenitra, Morocco.

[(b)]Laboratory of Separation Processes, Department of Chemistry, Faculty of Science, Ibn Tofail University, PO Box 133, 14000, Kenitra, Morocco.

[(c)] Agro-Resources, Polymers and Process Engineering Laboratory, Department of Chemistry, Faculty of Science, Ibn Tofail University, P.O. Box 133, 14000, Kenitra, Morocco.

[(d)] Regional Center for Education and Training Professions (CRMEF), Kenitra, Morocco.

[(e)] Materials, Nanotechnology and Environment Laboratory, Faculty of Sciences, Mohammed V University, Av. Ibn Battouta, P.O. Box 1014 Agdal-Rabat, Morocco.

* *Corresponding author:*
touir8@gmail.com
Received 07 Jan 2020,
Revised 25 Jan 2020,
Accepted 09 Feb 2020.

Abstract

The adsorption behaviour of (3aR,6aR)-2,2-dimethyl-6-(octyloxy)-5-(oxiran-2-yl) tetrahydrofuro[2,3-d][1,3]dioxole (EGC8) and (3aR,5R,6R,6aR)-2,2-dimethyl-5-((S)-oxiran-2-yl)-6 (tetradecyloxy) tetrahydrofuro[2,3-d][1,3]dioxole (EGC14) as inhibitors for mild steel corrosion in 1M HCl have been investigated computationally using DFT ($DMol^3$) calculations with the GGA functional and DNP as the base set. DMol3 calculations were centered on the neutral forms of the molecules tested, since these types of inhibitors are impossible to be protonated in an acidic environment. Quantum chemical descriptors inform that tensioactives are more chemically reactive and the local and global reactivity is concentrated in the heads of these species. Fukui indices were determined to evaluate the nucleophilic and electrophilic centers of the atoms of the molecule. The molecular dynamics (MD) simulation used show that EGC8 and EGC14 inhibitors are located vertically in relation to the surface. The values of $E_{interaction}$ and $E_{binding}$ reflect the spontaneity of the adsorption process.

Keywords: *Epoxy glucose derivatives; Mild steel; adsorption; DFT;* $DMol^3$*;* MD

1.Introduction

Several families of organic molecules are frequently used as corrosion inhibitors, firstly to protect a metal, and secondly to understand the mechanism of action of these inhibitors on a metal surface [1-7]. Indeed, the most useful metal in the field of industry is carbon steel (iron-based). These industries are in contact with atmospheres in which acids are commonly used for pickling, oil well acidification and other uses, which leads to corrosion of the metal [8,9]. In order to solve this scourge, it is necessary to use more performant and efficient organic inhibitors to battle this phenomenon [10]. The degree of efficacy of the inhibitory molecules depends on several very important factors, among them, Heterocyclic and aromatic compounds contain heteroatoms such as S, N and O, which are coupled with electron donor groups either by the mesomeric or inductive effect [11-13]. This frequently leads to the best adsorption on the metal surface by the phenomenon of electron sharing towards empty gaps (vacant d-orbitals) located on this surface. As a result, the formation of stronger bonds promotes the protection of the metal of interest. The majority of tensioactives, they are used as corrosion inhibitors, these species are characterized by a chemically active polar head and a linear chain often carbonaceous[14-16]. Various scientific research works in the domain of corrosion inhibition indicate that tensioactives interact with the metal surface through the motif which is very active (Head). In this context, the compounds studied in work namely (3aR, 6aR)-2, 2-dimethyl-6-(octyloxy)-5-(oxiran-2-yl)tetrahydrofuro[2, 3-d][1, 3]dioxole (EGC8) and (3aR, 5R, 6R, 6aR)-2,2-dimethyl-5-((S)-oxiran-2-yl)-6-(tetradecyloxy)tetrahydrofuro[2, 3-d][1, 3]dioxole (EGC14) (Figure1) behave as tensioactives with very large carbon chains. The theoretical methods used to explain the chemical reactivity of the inhibitors tested with the metal surface are chemical quantum calculations using DMol^3 and molecular dynamics simulations for correlating the results obtained with experimentally determined values of corrosion inhibitory efficiencies.

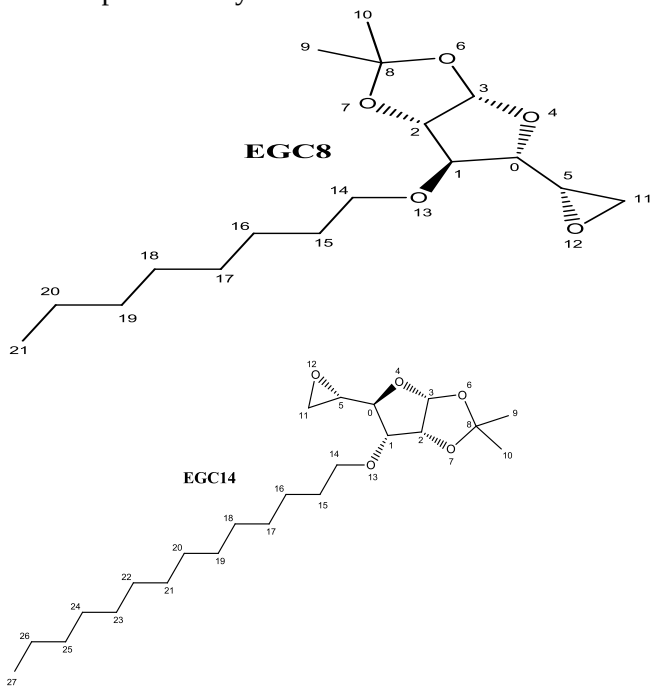

Figure1: Chemical structure of the molecules studied

2.Details of quantum chemical calculations and MD simualtions

The necessary object of this work is to understand the mode of action of an inhibitory molecule on the metal surface, theoretical studies, i.e. quantum chemical calculation and molecular dynamics (DM) simulation, remain among the most widely used methods to explain this phenomenon [17,18]. The theoretical method based on DMol^3 was used to determine the electron density of frontier molecular orbitals (FMO) in order to determine the main quantum chemical

descriptors namely the energy of the highest molecular orbital (E_{HOMO}) and the lowest molecular orbital (E_{LUMO}), the energy gap ($E = E_{LUMO}-E_{HOMO}$), the number of electrons transferred (ΔN_{110}), the dipole moment (μ) and the total energy (TE) [19-21]. We have chosen the theory of Dmol^3 with the method of BLYP /GGA and DNP as the base set. This is done using Material Studio 8.0 [22]. To describe in detail the difference in inhibition efficiency between the two molecules examined. To visualize the general appearance of the adsorption of EGC8 and EGC14 on the steel surface, we need to use molecular dynamics (MD) simulation. This simulation was carried out by Forcite module placed in the Material Studio 8.0 [22]. The interaction phenomena between the monomers and Fe (110) surface were simulated in a three-dimensional box 27.30* 27.30* 37.13 Å^3 with a vacuum of 25 Å, using the COMPASS force field with a periodic condition [23]. The chemical species inserted in the vacuum are an inhibitory molecule monomer for each simulation, 500 water molecules, 5 Cl^- anions and 5 H_3O^+ cations. The crystalline cells was exposed to the NVT in the simulation time of 400 ps which was achieved with the simulated temperature of 298 K using the Andersen thermostat [24].

The interaction ($E_{interaction}$) and binding ($E_{binding}$) energies of system- inhibitor are determined as follows [25]:

$$E_{interaction} = E_{total} - (E_{surface+solution} + E_{inhibitor}) \quad (1)$$

$$E_{binding} = - E_{interaction} \quad (2)$$

Where E_{total} is the total energy of the whole studied system, $E_{surface+solution}$ is referred to the total energy of Fe (110) surface and solution without the inhibitor and $E_{inhibitor+solution}$ represents the total energy of inhibitor and solution, and $E_{solution}$ is the total energy of the solution

3. Results and discussions

3.1. EIS study

The technique of electrochemical impedance spectroscopy assists us in understanding the reactions that take place at the inhibitor/metal interface [26]. The electrochemical parameters obtained from the simulations using the equivalent electrical circuit (Figure 2) of the EGC8 and EGC14 inhibitors are collected in Table 1.

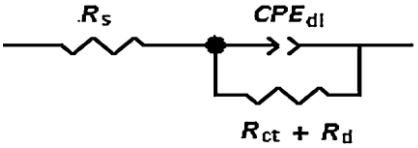

Figure 2: Equivalent electrical circuit suitable

Inhibitory efficacy (η_{EIS}) is calculated by the following formula:

$$\eta_{EIS} = \frac{R_p - R_p^0}{R_p} \times 100 \quad (3)$$

Where R_p^0 and R_p are the resistance polarization values without and with inhibitor, respectively. The electrochemical parameters are already discussed and interpreted in part I. Moreover, the efficiency values mentioned in Table 1 show that they increase with concentration, attaining 93.20% for EGC8 and 93.48% for EGC14 at 10^{-3}M. As we have found that these two efficacy values are close to each other, reflecting the fact that these two inhibitors have the same mode of action on the metal surface. To confirm this result, we conducted a more detailed theoretical study, namely the theory of density functional theory (DMol^3) and molecular dynamics simulation.

Table 1: Electrochemical parameters for mild steel in 1 M HCl with various concentrations of EGC8 and EGC14 at 298 K

Inhibitors	C (M)	R_s(Ω cm^2)	$R_{ct}+R_d$(Ω cm^2)	C_{dl}(µF cm^{-2})	η_{EIS} (%)
Blank solution	1M	2.08±0.03	32.41±0.78	128.1±0.66	-
EGC8	10^{-6}	2.66±0.05	130.01±0.64	54.91±0.21	84.03
	10^{-5}	1.46±0.03	339.70±0.43	67.63±0.41	86.72
	10^{-4}	1.68±0.01	673.20±0.44	40.73±0.34	90.06
	10^{-3}	1.65±0.02	768.10±0.43	41.06±0.31	93.20
EGC14	10^{-6}	0.43±0.05	53.39±0.36	11.05±0.31	84.26
	10^{-5}	0.88±0.03	320.40±0.44	48.66±0.08	88.39
	10^{-4}	1.65±0.14	545.51±0.43	40.66±0.54	90.66
	10^{-3}	2.15±0.19	871.00±0.40	56.04±0.18	93.48

3.2. DMmol^3 theory of neutral inhibitors

The degree of structure of an organic molecule is considered among the factors influencing the inhibiting efficiency against corrosion [27]. The molecules studied (EGC8 and EGC14) in this work have significant linear carbon chains that are related with the same functional motif. If for that reason we can consider these molecules as tensioactives. With state-of-the-art quantum chemical calculations, we determined the regions responsible for the local and global activities of the tested molecules. Therefore, we can predict the adsorption processor of these species on the surface of the steel under study. Figure 3 shows the optimized structures of the EGC8 and EGC14 molecules with the minimum energies of each compound, reflecting the stabilized state of these molecules. Moreover, it is very noticeable that the two molecules have the same number of optimization steps (20 optimization steps), which shows that these species stabilize with the same optimization cycle. In the same way, the values of the minimum energies in Hartree are negative reflecting that these optimized molecules have very important chemical reactivities [28]. consequently the EGC14 molecule has taken the minimum value of the total energy of -1277.731Ha and lower than the EGC8 value (1041.916 Ha). Which indicates that EGC14 is chemically more reactive than EGC8.

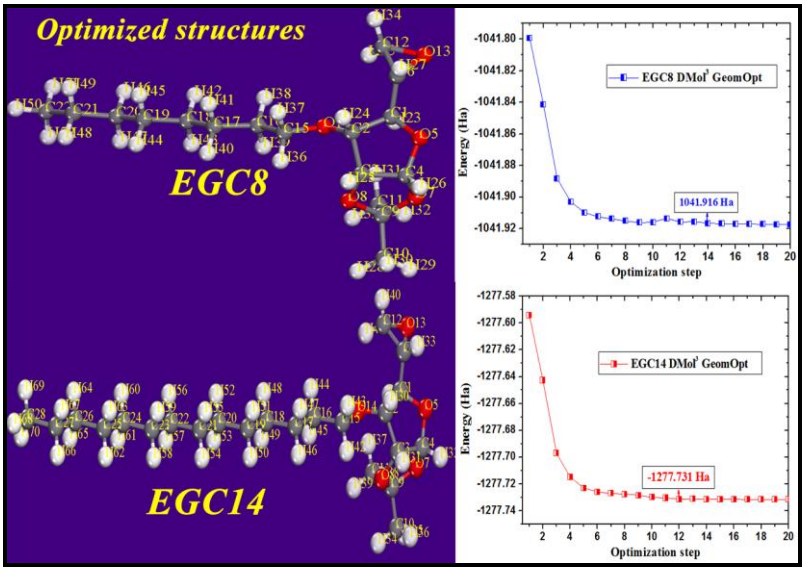

Figure3: Optimized structures of the EGC8 and EGC14 with the total énergie in Hartree

In general, in an organic molecule, the regions covered by the electronic densities of FMO (HOMO or LUMO) are capable of reacting with the iron atoms existing on the surface of steel [29]. Such as, regions that have a HOMO electron density, they are available to share their electrons with the vacant orbitals located in the metal surface, leading to the formation of covalent bonds [30]. Conversely, regions containing LUMO electron density are prepared by the retrodonation effect to receive electrons from the filled core layers [31]. Indeed, this behavior favors the adsorption of the studied molecule on the surface of the substrate. In this context, Figure 4 shows the special electron density distribution of the FMOs of EGC8 and EGC14 molecules. It is interesting to note that the electron density of FMOs is localized on the same pattern that carries oxygen atoms and heterocycles. This shows that this motive is responsible on the donor-acceptor property and the majority of the active sites are located in this part. While the carbon chain carries no electronic trend. This result allows concluding that the part recovered by the electronic density HOMO el LUMO is possibly adsorbed on the contact surface.

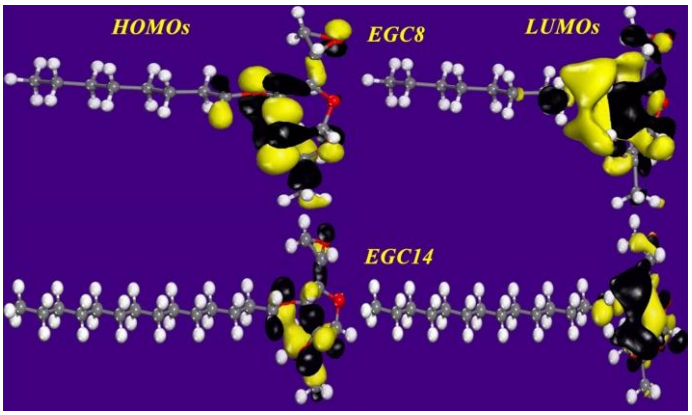

Figure4: Topographic distributions of the electron density of the FMO orbitals of EGC8 and EGC14 neutral molecules

Table 2: Quantum chemical descriptor distributions of EGC8 and EGC14 neutral molecules

Molecules	**E_{HOMO} (eV)**	**E_{LUMO} (eV)**	**ΔE_{gap} (eV)**	**ΔN_{110}**	**μ (D)**	**ET (Ha)**
EGC8	-5.665	-0.563	5.102	0.334	4.405	-1041.916
EGC14	-5.655	-0.566	5.088	0.336	4.451	-1277.731

Table 2 compiles the main quantum chemical descriptors used to explain the order of inhibitory efficacy between the two molecules studied [32]. The facility of the adsorption mechanism and the high chemical reactivity of the EGC14 inhibitor molecule on the steel surface could be due to the low value of the energy difference (ΔE_{gap}) (5.0885 eV), the high value of E_{HOMO} (-5.655 eV), and lowest value of E_{LUMO} (-0.5665 eV), the high value of dipole moment (4.451D) and the high value of electron number transferred (ΔN_{110}) (0.336) according to Lukovit [33]. These results show that the EGC14 inhibitor better protects the metal surface by blocking the majority of the active sites existing in the substrate surface, in order to decrease the degradation rate of this metal. In addition, the influence of the carbon chain increase effectively leads to an increase in the inhibitory capacity of EGC14. The theoretical calculation data obtained are completely agreed with the experimental results, confirming that the inhibitory performance of EGC14 is higher than that of EGC8. Local reactivity was assessed by calculating the Fukui indices; these sites make it possible to determine which atoms are responsible for the electrophilic and nucleophilic attacks of each inhibitor molecule [34].

The high values of the condensed Fukui functions f_K^+ and f_K^- represent the electron acceptor and donor sites, respectively. Often the most relevant sites are located in the HOMO (f_K^-) and LUMO (f_K^+) electron density distribution [35].

Table3: Condensed Fukui functions on C and O atoms of the EGC8 and EGC14 in their no-protonated form in the gaseous phase using GGA/BLYP/DNP

Atoms	**EGC8**		**EGC14**	
	f_K^+	f_K^-	f_K^+	f_K^-
C (1)	0.025	0.009	0.021	0.011
C (2)	0.048	0.031	0.049	0.031
C (3)	0.055	0.036	0.054	0.036
C (4)	0.032	0.014	0.029	0.017
O (5)	0.025	0.084	0.030	0.089
C (6)	0.016	0.008	0.013	0.010
O (7)	0.030	0.055	0.030	0.069
O (8)	0.040	0.045	0.038	0.043
C (9)	0.015	0.018	0.013	0.019
C (10)	0.017	0.030	0.017	0.028
C (11)	0.014	0.024	0.012	0.026
C (12)	0.025	0.020	0.022	0.022
O (13)	0.040	0.071	0.041	0.069
O (14)	0.039	0.043	0.037	0.047
C (15)	0.032	0.015	0.033	0.014
C (16)	0.006	0.004	0.008	0.003
C (17)	0.003	0.005	0.004	0.004
C (18)	0.003	0.002	0.003	0.002
C (19)	0.002	0.002	0.002	0.002
C (20)	0.002	0.001	0.002	0.001
C (21)	0.002	0.002	0.001	0.001
C (22)	0.001	0.003	0.001	0.001
C (23)			0.001	0.001
C (24)			0.001	0.000
C (25)			0.000	0.000
C (26)			0.000	0.000
C (27)			0.000	0.001
C (28)			0.001	0.001

Indeed, Table 3 regroups all the values of the Fukui indices. According to this table the C (2) and C (3) atoms of two compounds EGC8 and EGC14 have the high value of f_K^+, which means that these sites are available to receive electrons from the electron donor group. These two atoms are located in the active part of the molecule which carries electron density distributed over its skeleton. While the O (5), O (7) and O (13) atoms of two studied compounds are

responsible for the electrophilic attack, permitting the sharing of their electrons with the empty orbitals of the iron atoms through the formation of the stronger bonds. Oxygen atoms belonging to the active part of the mentioned molecules are possibly responsible for the inhibitory properties of these molecules. The active sites located in the carbon chain have very low values of f_K^+ and f_K^- condensed functions, which shows that this chain is unable to adsorb on the substrate surface.

3.2. DM simulation

In order to further explain and understand the adsorption process of selected inhibitor molecules on the steel surface, we used the method of molecular dynamics simulation [36]. This method makes it possible to evaluate the interatomic interactions between the atoms and heteroatoms of the molecules under investigation and iron atoms. Indeed, the crystalline cell has been built and filled by species similar to those used in the experimental part, that's why we have created a system very close to the real condition. Using this system, we studied the behavior of EGC8 and EGC14 molecules in the acidic medium in relation to the iron surface. Figure 5 shows images of the top and side views of the adsorption configuration of EGC8 and EGC14 monomers on the metal surface. From this figure, we found that the inhibitory molecules adsorb through the active function which carries heterocyclic, while the carbon chain of two compounds is oriented upwards. These visual observations show that both compounds behave as tensioactives. These species act in the same way, resulting in a small energy difference between the two adsorbed compounds (Table 4). Therefore, the active sites determined by the Fukui indices are well adsorbed on the metal surface, which shows that all these data obtained by the simulation confirm the results discovered by the quantum chemical calculation.

The values of energy potentials such as interaction and binding energy of the systems studied are collected in Table 4. As we have noticed that the negative and very close together values of interaction energy of two selected molecules show the spontaneity of the adsorption process [37]. In addition, the positive values of the adsorption energy reflect the strong adsorption of EGC8 and EGC14 on the metal surface [38]. These simulation results confirm the order of the inhibitory efficacy observed experimentally.

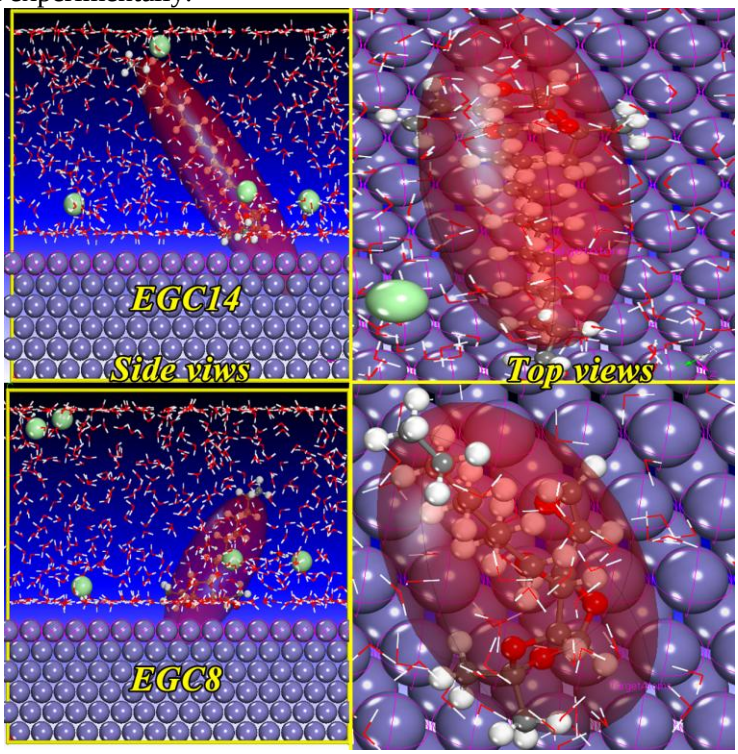

Figure 5: Equilibrated adsorption configurations of EGC8 and EGC14 from Fe (110) surface at 298K

Table4: $E_{interaction}$ and $E_{binding}$ energies for EGC8 and EGC14 on Fe (110) surface at 298 K, all values in Kj mol^{-1}

System-inhibitors	$E_{interaction}$	$E_{binding}$
System-EGC8	-233.459	233.459
System-EGC14	-246.563	246.563

To assess the nature of the bonds formed between the atoms and heteroatoms of the inhibitor molecules and the iron atoms of the metal surface, we used a method derived from molecular dynamics simulation such as radial distribution function (RDF) [39]. The RDF is determinate as follows:

$$g_{XY}(r) = \frac{1}{\langle \rho_Y \rangle_{local}} \times \frac{1}{N_X} \sum_{i \in X}^{N_X} \sum_{i \in Y}^{N_Y} \frac{\delta(r_{ij} - r)}{4\pi r^2} \qquad (4)$$

The g (r) functions give the density probability for an atom of the X particle to have a neighbor of the Y particle at a given interatomic distance r. Moreover, $\langle \rho_Y \rangle_{local}$ means the species density of Y averaged over all shells around X species. In our study, we just based on the oxygen atoms O5, O7 and O13 considered as the most favorable sites for electrophilic attacks as indicated in the part of the local reactivity (Fukui indices). The results obtained by the MD simulation are shown in Figure 6 the cell ambient temperature. This figure indicates that the RDF values for the surfactant molecules studied are noted on the first most intense peak for each heteroatom/Fe spectrum. It is very interesting to observe that all RDF distance values are less than 3.5 Å, indicating that the selected species form coordinative bonds with the iron atoms of the first layer [40]. We also noticed that the RDF values of EGC14 compound are lower than those found in the case of the EGC14 molecule, resulting in EGC14 adsorbing better on the metal surface by forming a more efficient protective layer.

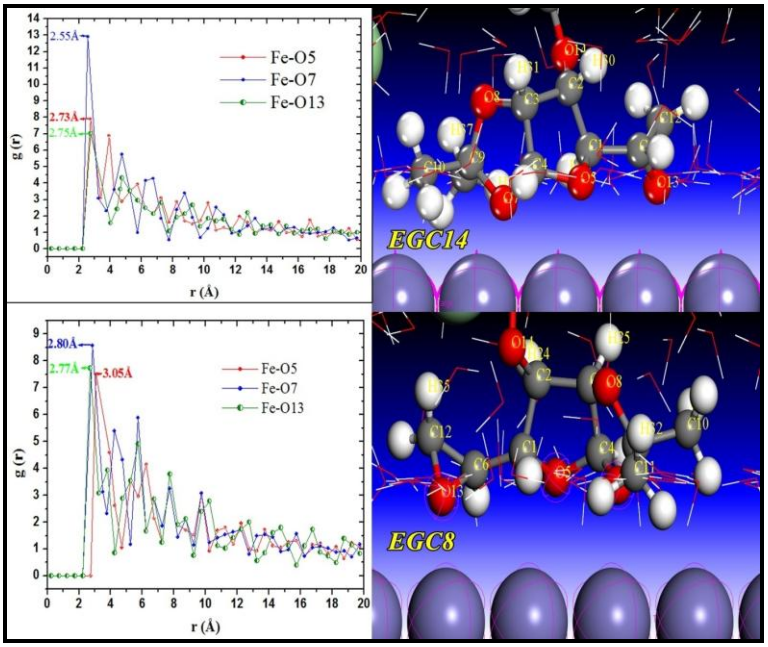

Figure 6: *RDF* functions for EGC8 and EGC14 on Fe (110) surface at 298 K

4. Conclusion

The results obtained from the theoretical calculations are given as follows:

✓ All descriptors computed in the neutral form of the molecules studied strongly suggested that the two species have the same behavior, which correlates with the experimental data;

✓ Our inhibitors are adsorbed by the active function, indicating that these molecules behave like tensoactives;

✓ The negative values of $E_{interaction}$ and the positive values of $E_{binding}$ show that the adsorption process of the studied compounds is exothermic and could occur spontaneously;

✓ The RDF function shows that the selected oxygen heteroatoms form covalent bonds with the iron atoms of the metal surface;

✓ A good agreement was found between theoretical and experimental results.

References

[1] S.A. El Wanees, M.I. Alahmdi, S. Rashwan, M. Kamel, M.A. Elsadek, *International Journal of Electrochemical Science*, 11 (**2016**) 9265-9281.

[2] A. El Assyry, B. Benali, B. Lakhrissi, M. El Faydy, M. Ebn Touhami, R. Touir, M. Touil, *journal of Research on Chemical Intermediates*, 41 (**201**5) 3419-3431.

[3] D. Ben Hmamou, R. Salghi, A. Zarrouk, H. Zarrok, R. Touzani, B. Hammouti, A. El Assyry, *Journal of Environmental Chemical Engineering*, 3 (**2015**) 2031-2041.

[4] H. Zarrok, S.S. Al-Deyab, A. Zarrouk, R. Salghi, B. Hammouti, H. Oudda, M. Bouachrine, F. Bentiss, *International Journal of Electrochemical Science* 7 (**2012**) 4047-4063.

[5] A. Zarrouk, H. Zarrok, Y. Ramli, M. Bouachrine, B. Hammouti, A. Sahibed-dine, F. Bentiss, *Journal of Molecular Liquids* 222 (**2016**) 239-252.

[6] A. Zarrouk, B. Hammouti, A. Dafali , M. Bouachrine, H. Zarrok, S. Boukhris, S.S. Al-Deyab, *Journal of Saudi Chemical Society* 18 (**2014**) 450-455.

[7] M. El Faydy, M. Galai, A. El Assyry, A. Tazouti, R. Touir, B. Lakhrissi, M. Ebn Touhami, A. Zarrouk, *Journal of Molecular Liquids* 219 (**2016**) 396-404.

[8] M.S. Morad, A.M.K. El-Dean, 2,2′-Dithiobis(3-cyano-4,6-dimethylpyridine): A new class of acid corrosion inhibitors for mild steel, *Journal of Corrosion Science*, 48 (**2006**) 3398-3412.

[9] R. Hsissou, O.Dagdag , S.Abbout , F. Benhiba , M. Berradi , M. El Bouchti ,A.Berisha , N.Hajjaji , A. Elharfi, *Journal of Molecular Liquids*, 284(**2019**) 182–192

[10] M. Hosseini, S.F.L. Mertens, M. Ghorbani, M. R. Arshadi, *Journal of Materials Chemistry and Physics*, 78 (**2003**) 800-808.

[11] P. Lowmunkhong, D. Ungthararak, P. Sutthivaiyakit, *Journal of Corrosion Science*, 52 (**2010**) 30-36.

[12] F. Bentiss, C. Jama, B. Mernari, H. E. Attari, L. El Kadi, M. Lebrini, M. Traisnel, M. Lagrenee, *Journal of Corrosion Science*, 51 (**2009**) 1628-1635.

[13] L. B. Tang, X. Li, L. Li, G. Mu, G. Liu, *Journal of Surface and Coatings Technology*, 201 (**2006**) 384-388.

[14] M. Lashkari, M. R. Arshadi, *Journal of Chemical Physics*, 299 (**2004**) 131-137.

[15] B.B. Damaskin, O.A. Petrii, V.V. Batrakov, Plenum Press, *New York*, **1971**.

[16] W. Linderink, M.V.D. Linden, J.H.W. Wit, *Journal of Corrosion Science*, 38 (**1993**)1989.

[17] A. Ramazani, M. Sheikhi, H.Yahyaei, *Journal of Chemical Methodologies*, 1(**2017**)28-48.

[18] R. Nabah, F. Benhiba, Y. Ramli, M. Ouakki, M. Cherkaoui, H. Oudda, R. Touir, I. Warad and A. Zarrouk, *Journal of Analytical & Bioanalytical Electrochemistry* , 10(10)(**2018**)1375-1398.

[19] M. Khattabi , F. Benhiba , S. Tabti, A. Djedouani, A. El Assyry, R. Touzani, I. Warad, H. Oudda, A. Zarrouk, *Journal of Molecular Structure*, 1196 (**2019**)231-244.

[20] H.Tanak, A. Ağar, M.Yavuz, *Journal of* Molecular Modeling, 16(3)(**2010**) 577-587.

[21] V. Sastri, J. Perumareddi, Molecular orbital theoretical studies of some organic corrosion inhibitors, *Journal of Corrosion*, 53 (**1997**) 617-622.
[22] Materials Studio, Revision 8.0, Accelrys Inc., San Diego, USA (**2016**).
[23] H. Sun, *Journal of Physical Chemistry*, B102 (**1998**) 7338-7364.
[24] H.C. Andersen, *Journal of Physical Chemistry*, 72 (1980) 2384-2393.
[25] M. Rbaa, F. Benhiba, I.B. Obot, H. Oudda, I. Warad, B. Lakhrissi, A. Zarrouk, *Journal of Molecular Liquids*, 276 (**2019**) 120 –133.
[26] R. Yildiz, *Journal of Corrosion Science*, 90 (**2015**) 544–553.
[27] F. Benhiba, Y. ELaoufir, M. Belayachi, H. Zarrok, A. El Assyry, A. Zarrouk, B. Hammouti, E. E. Ebenso, A. Guenbour, S. S. Al Deyab, H. Oudda, *Journal of Der Pharmacia Lettre*, 6 (4) (**2014**) 306-318.
[28] L.O. Olasunkanmi, M.M. Kabanda, E.E. Ebenso, *Physica E Low Dimens. Syst. Nanostruct*. 76 (**2016**) 109-126.
[29] H. Serrar, M. Galai, F. Benhiba, M. Ouakki, Z. Benzekri, S. Boukhris, A. Hassikou, A. Souizi, H. Oudda, M. Ebn Touhami, *Journal of Chemical Technology and Metallurgy*, 53 (3)(**2018**) 597-605.
[30] L. Reznik, L. Sathler, M.Cardoso, *Journal of Material Corrosion*, 59 (**2008**) 685-690.
[31] F. Benhiba, H. Zarrok, A. Elmidaoui, M. El Hezzate, R. Touir, A. Guenbour, A. Zarrouk, S.Boukhris, H.Oudda, *Journal of Materials and Environmental Sciences*, 6 (8)(**2015**) 2301-2314.
[32] S. Javadian, B. Darbasizadeh, A.Yousefi, F. Ektefa, N. Dalir, J. Kakemam. *Journal of the* Taiwan Institute *of Chemical Engineers*, 71(**2017**)344–54.
[33] I. Lukovits, E. Kalman, F. Zucchi, Journal of Corrosion, 57 (**2001**) 3.
[34] T. Laabaissi, F. Benhiba, Z. Rouifi, M. Rbaa, H. Oudda, H. Zarrok, B. Lakhrissi, A. Guenbour, I. Warad, A. Zarrouk, *Journal of Protection of Metals and Physical Chemistry of Surfaces*, 5(**2019**) 1–15.
[35] K. Cherrak, F. Benhiba, N.K. Sebbar , E.M. Essassi, M. Taleb, A. Zarrouk, A. Dafali, *Journal of Chemical Data Collections*, 22 (**2019**) 100252.
[36] Y. Tang, X. Yang, W. Yang, Y. Chen, R. Wan, Journal of Corrosion Science, 52 (**2010**) 242-249.
[37] S.K. Saha, P. Ghosh, A. Hens, N.C. Murmu, P. Banerjee, *Physica E*, 66 (**2015**) 332-341.
[38] M. El Faydy, F. Benhiba, B. Lakhrissi, M. Ebn Touhami, I. Warad, F. Bentiss, A. Zarrouk, *Journal of Molecular Liquids*, 295 (**2019**) 111629.
[39] A. El yaktini, A. Lachiri, M. El Faydy, F. Benhiba, H. Zarrok, M. El Azzouzi, M. Zertoubi, M. Azzi, B. Lakhrissi and A. Zarrouk, *Journal of International Journal of Corrosion and Scale Inhibition*, 7(4) (**2018**) 609–632
[40] P. Naeiji, F.Varaminian, M. Rahmati, Comparison of the Thermodynamic, Structural and Dynamical Properties of Methane/Water and Methane/Water/Hydrate Systems Using Molecular Dynamic Simulations, *Journal of Natural Gas Science and Engineering*,(**2017**). 10.1016/j.jngse.2017.04.010